

1
2
3
4 **Coadaptation of the chemosensory system with voluntary**
5 **exercise behavior in mice**

6
7
8
9 Quynh Anh Thi Nguyen¹, David Hillis², Sayako Katada³, Timothy Harris², Crystal Pontrello⁴,
10 Theodore Garland, Jr.^{1,2,5} and Sachiko Haga-Yamanaka^{1,2,4*}

11
12 ¹ Neuroscience Graduate Program, University of California Riverside, Riverside, California, USA

13 ² Graduate Program in Genetics, Genomics & Bioinformatics, University of California Riverside,
14 Riverside, California, USA

15 ³ Department of Stem Cell Biology and Medicine, Graduate School of Medical Sciences, Kyushu
16 University, Fukuoka, Fukuoka, Japan

17 ⁴ Department of Molecular, Cell, and Systems Biology, University of California Riverside,
18 Riverside, California, USA

19 ⁵ Department of Evolution, Ecology and Organismal Biology, University of California Riverside,
20 Riverside, California, USA

21

22 *Corresponding author

23 Email: sachikoy@ucr.edu

24

25 **Abstract**

26 Ethologically relevant chemical senses and behavioral habits are likely to coadapt in response
27 to selection. As olfaction is involved in intrinsically motivated behaviors in mice, we hypothesized
28 that selective breeding for a voluntary behavior would enable us to identify novel roles of the
29 chemosensory system. Voluntary wheel running (VWR) is an intrinsically motivated and naturally
30 rewarding behavior, and even wild mice run on a wheel placed in nature. We have established 4
31 independent, artificially evolved mouse lines by selectively breeding individuals showing high VWR
32 activity (High Runners; HRs), together with 4 non-selected Control lines, over 88 generations. We
33 found that several sensory receptors in specific receptor clusters were differentially expressed between
34 the vomeronasal organ (VNO) of HRs and Controls. Moreover, one of those clusters contains multiple
35 single-nucleotide polymorphism loci for which the allele frequencies were significantly divergent
36 between the HR and Control lines, i.e., loci that were affected by the selective breeding protocol.
37 These results indicate that the VNO has become genetically differentiated between HR and Control
38 lines during the selective breeding process. Although the role of the vomeronasal chemosensory
39 receptors in VWR activity remains to be determined, the current results suggest that these
40 vomeronasal chemosensory receptors are important quantitative trait loci (QTLs) for voluntary
41 exercise in mice. We propose that olfaction may play an important role in motivation for voluntary
42 exercise in mammals.

43

44

45 **Introduction**

46 Chemical senses are involved in many aspects of behavior. Olfaction is especially
47 important for controlling such intrinsically motivated behaviors as food-seeking, social
48 interactions, and reproductive- and fear-driven behaviors (1). An ethologically relevant cue is
49 sensed by chemosensory receptors expressed in the sensory organs, which activate a specific
50 neural circuitry for behavioral motivation and induces an appropriate behavioral output in a
51 specific context (2-5). Comparative functional studies involving insect model species propose a
52 model wherein molecular evolution of chemosensory receptors is sufficient to induce changes in
53 neural circuit activity and behavioral patterns (6). Thus, ethologically relevant cues, receptors,
54 neural circuitries, and behavioral habits are likely to evolve together (coadapt) in response to
55 natural and sexual selection.

56 One olfactory organ, the vomeronasal organ (VNO), occurs in some amphibians,
57 squamates, and some mammals, including rodents. The VNO is known to detect intraspecific
58 signals known as pheromones that trigger behavioral and physiological changes in receivers (7).
59 Pheromones are non-volatile peptides and small molecular weight compounds that are excreted in
60 such fluids as urine and tears. These molecules are taken up from the environment to the VNO by
61 direct contact and activate the vomeronasal sensory neurons (VSNs) (8, 9). Generally, each VSN
62 expresses a member of the vomeronasal receptor families: *type 1 vomeronasal receptors*
63 (*Vmn1rs*), *type 2 vomeronasal receptors* (*Vmn2rs*), and *formyl peptide receptors* (*Fprs*), with
64 some exceptions (10-14). The signals detected by these receptors in the VSNs are axonally sent to
65 glomerular structures and synaptically transmitted to the postsynaptic neurons, also known as
66 mitral-tufted cells, in the accessory olfactory bulb (AOB) (15, 16). The signals are then processed

67 in the amygdala and hypothalamus, which induce the animal's instinctive behavioral responses
68 and endocrinological changes (7, 17, 18).

69 Rapid evolution of the receptor genes is a pronounced feature of the vomeronasal system
70 (19-32). Different species of animals have divergent family members of vomeronasal receptor
71 genes (24, 27-29, 33, 34). Even within the *Mus musculus* (house mouse) species complex,
72 variation in the coding sequence is frequently observed (19). Moreover, the abundance of receptor
73 genes expressed in the VNO varies even among different inbred mouse strains (35). Distributions
74 of single nucleotide polymorphisms (SNPs) observed in lab-derived strains are non-random, and
75 correlated with vomeronasal receptor phylogeny as well as genomic clusters (19). These
76 observations led us to hypothesize that selective breeding for a behavior that is modulated by
77 chemosensory signals would induce an alteration in genomic clusters of vomeronasal receptors
78 that are potentially involved in the behavior.

79 Voluntary wheel running (VWR) is an intrinsically motivated behavior, and even wild
80 mice run on a wheel placed in nature (36). Notably, VWR is one of the most widely studied
81 behaviors in laboratory rodents (37-39). Individual differences in VWR are highly repeatable on a
82 day-to-day basis, the trait is heritable within outbred populations of rodents, and genes and
83 genomic regions associated with VWR are being identified (40). Moreover, some of the
84 underlying causes of variation in VWR have been elucidated, in terms of both motivation and
85 ability for voluntary exercise (38, 41, 42). Importantly, a previous study demonstrated that the
86 presence of conspecific urine increased VWR activity level in adult wild-derived mice (43),
87 suggesting that external chemosensory cues also have a modulatory role in VWR activity.

88 We have established 4 independent, artificially evolved mouse lines by selectively
89 breeding individuals showing high VWR activity (High Runners; HRs), along with 4 independent,

90 non-selected Control lines over 88 generations (44, 45). Briefly, all 4 HR lines run ~2.5–3.0-fold
91 more revolutions per day as compared with the 4 Control lines (46, 47). Studies of mice allowed
92 access to clean wheels or those previously occupied by a different mouse revealed that HRs show
93 higher sensitivity to previously-used wheels and display greater alteration in daily wheel running
94 activities than the Controls (48). This result suggests that selective breeding for high running
95 activity was accompanied by altered sensitivity to other individuals, suggesting a potential
96 coadaptation of the chemosensory system with voluntary wheel running.

97 In this study, we examined whether selective breeding for VWR has differentiated the
98 vomeronasal receptor genes between HR and Control lines. We found that a repertoire of receptor
99 genes was differentially expressed between the VNO of HR and Control lines, which resulted
100 from reduction or increase of specific vomeronasal receptor-expressing cells in the VNO of HR
101 lines. We also found that this gene expression change was partially due to the genetic alteration
102 upon selective breeding for VWR, suggesting a relationship between high running activity and the
103 function of the VNO in HR lines. Taken together, our results indicate vomeronasal receptors as
104 QTL for voluntary exercise behavior in mice.

105

106 **Results**

107 **Differential expression of vomeronasal receptors in the VNO of HR and Control lines**

108 To examine the impact of selective breeding for VWR activity on receptor gene expression
109 in the VNO, we conducted transcriptome analysis of the VNO from both males and females of HR
110 and Control lines. For each sex and replicate line of the 4 HR and 4 Control lines, total RNA
111 samples were prepared, each consisting of the combined VNOs from 3 individual mice. After

112 RNA sequencing, we identified 132 differentially expressed (DE) genes in the HR line group
113 compared to the Control line group (Figure 1). We identified 19 vomeronasal receptor genes in the
114 DE gene set, which belong to either the *Fpr*, *Vmn1r* or *Vmn2r* family (Figure 1, shown in red). Of
115 the 19 DE receptor genes, the Reads Per Kilobase Million (RPKM) of *Fpr3*, *Vmn2r8*, *Vmn2r9*,
116 *Vmn2r11*, *Vmn2r96*, *Vmn2r98*, *Vmn2r102* and *Vmn2r110* were significantly up-regulated, while
117 *Vmn1r188*, *Vmn1r236*, *Vmn2r15*, *Vmn2r16* and *Vmn2r99* were significantly down-regulated in the
118 VSNs of HR lines compared to Control lines (Figure 2A). The RPKM of *olfactory marker protein*
119 (*OMP*), which is abundantly and exclusively expressed in all mature VSNs in the VNO (49), was
120 not different between HR and Control lines (data not shown), indicating that receptor gene
121 expression changes were not due to variation in VSN number. The \log_2 fold change of
122 normalized expression of the DE genes varied from -3.3 to 2.1 (Figure 2B). *Fpr-rs4* and *Vmn2r16*
123 showed the largest upregulation and downregulation, respectively. To examine sexually-biased
124 expressions, we separated RPKMs of each DE receptor gene into sex and linetype groups
125 (Supplemental Figure 1) and performed a two-way ANOVA test to examine sex and linetype
126 differences. As shown in Supplemental Figure 2, *p* values for sexually-biased expression and
127 interaction were above 0.05 in all DE receptor genes, demonstrating that there are no sex-
128 dimorphic expression changes between HR and Control lines. These results suggest that
129 expression of the chemosensory receptor genes is differentially regulated in the VSNs between HR
130 and Control lines without a sex difference.

131 Interestingly, 15 out of 19 DE receptor genes are co-localized in specific vomeronasal
132 receptor clusters. *Vmn2r8*, *Vmn2r9*, *Vmn2r11*, *Vmn2r13*, *Vmn2r15*, and *Vmn2r16* are localize in a
133 ~1 Mb vomeronasal receptor cluster on chromosome 5, and *Fpr3*, *Fpr-rs4*, *Vmn2r96*, *Vmn2r98*,
134 *Vmn2r99*, *Vmn2r102*, *Vmn2r107*, *Vmn2r110*, and *Vmn1r236* are localized in a ~3 Mb

135 vomeronasal receptor cluster on chromosome 17 (Figure 3). *Vmn2r23*, *Vmn2r45*, *Vmn1r188*, and
136 *Vmn2r114* exist on chromosome 6, 7, 10, and 17, respectively (Figure 3), and they are surrounded
137 by vomeronasal receptors which are not differentially expressed between HR and Control lines.
138 These results suggest the correlation of differential expression of vomeronasal receptors and
139 genomic chromosomal locations, as well as other unknown causes.

140 **Accumulation of all-or-none SNPs in a vomeronasal receptor cluster**

141 We then hypothesized that differences between HR and Control lines in vomeronasal
142 receptor gene expression may be associated with differences in genomic sequences, especially
143 allele frequencies between HR and Control lines caused by the selective breeding. Previous
144 genome-wide SNP analysis detected 152 out of 25,318 variable SNP loci for which allele
145 frequencies are significantly different between HR and Control lines after correction for multiple
146 comparisons (50). As explained in the previous paper, the differentiation in allele frequencies for
147 these 152 loci cannot be attributed to random genetic drift. Of the 152 SNP loci, we particularly
148 focused on 61 loci that are fixed for the same allele in all 4 replicate HR lines but not fixed in any
149 of the 4 replicate Control lines, or vice versa (which we term “all-or-none SNPs”, Supplemental
150 table 1). The 61 SNP loci are not randomly distributed throughout the genome (Supplemental
151 Figure 3A). The majority of them (59 of 61) exist as a member of groups of 3 or more which are
152 located in close proximity on the genomic chromosomes (Supplemental Figure 3B). As a result,
153 only 11 all-or-none SNP clusters are observed in the genome (Supplemental Figure 3A)

154 Interestingly, 8 of the 61 all-or-none SNP loci are located in a ~3 Mb interval on
155 chromosome 17 that contains clusters of *Vmn1rs* (14), *Vmn2rs* (21), and *Fprs* (7) (Figure 4A).
156 Strikingly, 9 out of the 19 DE vomeronasal receptors are located in this all-or-none SNP cluster.
157 Five of the all-or none SNPs are localized near the differentially expressed vomeronasal receptors

158 (Fig 2B): SNP ID rs29503987 at 30 kb downstream and 20 kb upstream of *Fpr3* and *Fpr-rs4*,
159 respectively, rs33447983 at 8.4 kb downstream of *Vmn2r99*, rs6224641 at 30 kb downstream of
160 *Vmn2r99*, rs33649277 at 44 kb upstream of *Vmn2r102*, rs29522462 at 524 bp downstream of
161 *Vmn2r110*, and rs33120398 at the intron 1 of *Vmn2r110*. Other SNPs, such as rs33463529, are
162 also closely located near vomeronasal receptors, though changes in expression of the nearby
163 receptors were not observed. These results strongly suggest that changes in vomeronasal receptor
164 gene expression between HR and Control lines are at least partially caused by changes in allele
165 frequencies at multiple loci in response to selective breeding for VWR activity.

166 The rest of the DE vomeronasal receptors, which are located in another vomeronasal
167 receptor cluster on chromosome 5, as well as other solitary ones, are not surrounded by SNP loci
168 that are significantly differentiated between HR and Control lines (50). Therefore, expression
169 changes of the receptor genes may be mediated by SNPs that remain polymorphic in both lines, or
170 by different mechanisms.

171

172 **Differential number of *Fpr3*-expressing VSNs in the VNO of HR and Control lines**

173 To determine the significance at the cellular level in the VNO of the DE chemosensory
174 receptor genes, we chose one representative gene to determine whether there are differences in the
175 number of receptor-expressing VSNs, or alternatively, differences in transcript abundance in each
176 receptor-expressing VSN. We performed *in situ* hybridization to detect *Fpr3* in the VNO of 2-3
177 individual mice from each of the 4 HR and 4 Control lines, together with a probe for the *Gao*
178 (*Gnaol*). Expression of *Fpr3* is ~3 times higher in HR lines compared to Control lines in RNAseq
179 analysis (Figure 2B). Although *Fpr3*-expressing VSNs were observed in the VNO of both HR and
180 Control lines, the number of *Fpr3*-expressing VSNs in each VNO slice varied among lines (Figure

181 5A, B). In 3 Control lines (line 1, 4, and 5), *Fpr3* signal was barely observed in each VNO tissue
182 slice, while Control line 2 had a significantly higher number of *Fpr3*-expressing VSNs (Figure
183 5B). This result was consistent with the RNAseq data, in which the amount of *Fpr3* transcripts in
184 line 2 was higher than other Control lines (Figure 2A). We consistently observed multiple *Fpr3*-
185 expressing VSNs in most of the VNO tissue slices from the 4 HR lines and Control line #2 (Figure
186 5B, C). Generally, there were significantly more *Fpr3*-expressing VSNs in the HR versus the
187 Control lines (Figure 5C, Mann-Whitney test ($p < 0.05$)). The fluorescent intensity derived from
188 *Fpr3* gene transcripts in each VSN was not distinguishable between the VNO tissues from HR and
189 Control lines (Figure 5D and E). Taken together, these results demonstrate that the different
190 expression levels of the chemosensory receptors result from changes in the number of the
191 receptor-expressing VSNs. The results observed here are consistent with a previous finding in the
192 main olfactory system, which has a similar monoallelic pattern of receptor gene expression in each
193 sensory neuron (51): a positive correlation between tissue RNA levels of olfactory receptor genes
194 and numbers of OSNs expressing the receptors. Thus, the number of VSNs expressing specific
195 sets of chemosensory receptors are differentially regulated after selective breeding for VWR.

196

197 **Discussion**

198 In this study, we utilized a unique animal model: 4 replicate mouse lines that have been
199 experimentally evolved by selectively breeding individuals showing high VWR activity (HR
200 lines), along with their 4 independent, non-selected Control lines maintained over 88 generations
201 (44). The HR and Control lines provide a strong model for determining the contribution of
202 genetics to voluntary-exercise related traits (45, 52). In addition to the exercise ability-related
203 genetic adaptations found after selective breeding (38, 45), several changes at the level of the

204 central nervous system have also been identified, which contribute to elevation of VWR for HR
205 mice (38, 41, 53). Through SNP mapping analysis (Supplemental Fig 1), we found that 3 of the
206 61 all-or-none SNP loci that were fixed in all 4 replicate HR lines (but none of the 4 replicate
207 Control lines) were located in a genomic cluster exclusively containing T-box genes on
208 Chromosome 5. These genes are associated with GO terms of “bundle of His development,”
209 “embryonic forelimb morphogenesis,” “cardiac septum morphogenesis,” “ventricular septum
210 development,” and “cardiac muscle cell differentiation”. Indeed, compared with their 4 non-
211 selected Control line counterparts, mice from the 4 replicate HR lines have been shown to have
212 increased ventricular mass (46, 54-56), as well as altered cardiac functions (56-58). Thus, the
213 genome-wide SNP analysis of HR and Control lines of mice (50) could robustly identify QTL
214 associated with voluntary exercise behavior.

215 Vomeronasal receptors are among the most rapidly evolving genes in vertebrates (19-32).
216 Different taxonomic groups have divergent family members of vomeronasal receptor genes (22,
217 24, 27-29, 33, 34), and the abundance of receptor genes expressed in the VNO is different even
218 among inbred mouse strains (35). Moreover, many of the mouse pheromones identified as ligands
219 for vomeronasal receptors show strain specificity. For example, expression of the male pheromone
220 ESP1 is only observed in a few inbred strains, although males of wild-derived strains all secrete
221 abundant ESP1 peptide into their tears (59). Likewise, expression of juvenile pheromone ESP22 is
222 missing in some inbred strains (60). Major urinary proteins (MUPs) are potential ligands for
223 vomeronasal receptors, and all male mice of a given inbred strain secrete identical MUP members,
224 whereas wild-derived mice each exhibit a unique profile of emitted MUPs (61). Thus, pheromones
225 and vomeronasal receptors in the vomeronasal system may have evolved in response to various

226 environmental changes, including domestication, which resulted in alteration of coding sequences
227 and expression patterns.

228 Considering the extensive evolution of receptor genes, selective breeding for a
229 chemosensory-mediated behavior is an attractive alternative approach to reveal the functions of
230 vomeronasal receptors. VWR activity of a mouse strain that recently derived from the wild has
231 been shown to be increased by urinary chemosignals from other individuals (43). Therefore, if the
232 function of the VNO is involved in the modulation of VWR activity, then we would expect that
233 selective breeding for high VWR activity should impact vomeronasal receptors. Indeed, we found
234 that expression levels of several vomeronasal receptor genes as well as a few SNPs near the DE
235 receptor genes were different between HR and Control lines. Although the role of each DE
236 receptor in VWR activity needs to be determined in future studies, the current results suggest that
237 vomeronasal chemosensory receptors could be important QTLs for voluntary exercise in mice.

238 One of the important remaining questions is how the vomeronasal system modulates VWR
239 behavior in HR lines. One study measuring patterns of brain activity using c-Fos
240 immunoreactivity revealed multiple areas in the brain that appear to be associated with motivation
241 for VWR in HR lines (62). These areas include brain nuclei known to be motivation-related, such
242 as the prefrontal cortex, medial frontal cortex, and nucleus accumbens (NAc) (62). In addition, it
243 was recently shown in mice that VNO-mediated signals regulate the mesolimbic dopaminergic
244 system, especially by upregulating the ventral tegmental area (VTA)-NAc circuit, and that they
245 enhance reproductive motivation in mice (16). Thus, it is possible that the VNO-mediated
246 chemosensory signals also upregulate VWR activity by stimulating the VTA-NAc circuit.
247 Moreover, one of the hypothalamic targets of the vomeronasal system, the medial preoptic area
248 (MPOA), has been shown to regulate wheel-running activity in a hormone-dependent manner (63-.

249 66). It is therefore also conceivable that the VNO-mediated chemosensory signals upregulate
250 VWR by directly activating MPOA neurons. Combined with these previous observations, we
251 propose that chemosensory signals detected by the VNO activate specific areas of the central
252 nervous system that contribute to VWR activity. Future studies are expected to reveal the role of
253 the VNO in modulating physical exercise and other voluntary behaviors in rodents.

254

255 **Materials and Methods**

256 Animals

257 The experimental procedures were approved by the UCR Institutional Animal Care and
258 Use Committee and were in accordance with the National Institutes of Health Guide for the Care
259 and Use of Laboratory Animals. The VNOs studied were from 12-week old male and female mice
260 of 4 lines selected for high voluntary wheel running and 4 Control lines. The studied mice were
261 derived from generation 88 of a replicated selective breeding experiment for increased voluntary
262 wheel running behavior that began with a base population of the outbred Hsd:ICR strain (44).
263 Wheel revolutions were recorded in 1-minute intervals continuously for 6 days, and mice were
264 selected within-family for the number of revolutions run on days 5 and 6. In each selected HR
265 line, the highest-running male and female within 10 individual families were selected per
266 generation and each mouse was mated to a mouse from another family, within its line. This
267 within-family selection regimen minimized inbreeding such that the effective population size was
268 approximately 35 in each line (44). In the Control lines, one female and one male within each
269 family were chosen at random, though full sibling mating was again prevented. The mice in the
270 present study were neither full nor half-siblings.

271

272 RNA sequencing

273 The VNO tissues were harvested from 3 male and 3 female mice from each of the 4 HR
274 and 4 Control lines, immediately transferred to RNA later (Sigma-Aldrich), then stored at -80°C
275 until use for RNA-seq. VNO tissues from the same sex and line of mice were pooled and
276 homogenized in Trizol Reagent (Life Technologies, Carlsbad, CA) and processed according to the
277 manufacturer's protocol. Trizol-purified RNA samples were quantified using Qubit1 2.0 (Life
278 Technologies). The integrity of isolated RNA was measured by the 28S/18S rRNA analysis using
279 the Agilent 2100 Bioanalyzer (Agilent Technologies, Santa Clara CA) with RNA Nano chip
280 (Agilent Technologies, Palo Alto, CA). Samples had RNA integrity number values of at least 8.30.
281 Using the Ultra II Directional RNA Library Prep kit (NEB), each RNA sample was depleted of
282 ribosomal RNA and used to prepare an RNA-seq library tagged with a unique barcode at the UCR
283 IIGB Genomics Core. Libraries were evaluated and quantified using Agilent 2100 Bioanalyzer
284 with High Sensitivity DNA chip, then sequenced with the Illumina NextSeq 500 system (Illumina,
285 San Diego, CA, USA) and 75nt-long single-end reads were generated at the UCR IIGB Genomics
286 Core. A total of 8 libraries (4 HR lines and 4 Control lines) were multiplexed and sequenced in a
287 single lane which yielded ~11,000 M reads, averaging ~1,400 M reads per sample.

288 The RNA-seq data files are available in the National Center for Biotechnology Information
289 Gene Expression Omnibus (GEO) database (accession identifier GSE146644).

290

291 Differential gene expression analysis

292 The analysis compared the transcriptome profiles from both males and females of the HR
293 and Control lines of mice. Quality control of the sequence reads included a minimum average
294 Phred score of 30 across all positions using FastQC. Sequencing reads were aligned to the mouse
295 reference genome (GRCm38/mm10), using STAR aligner ver. 2.6.1d (67) with an increased
296 stringency unforgiving any of mismatches per each read ('-outFilterMismatchNmax 0'). Any reads
297 that map to multiple locations in the genome are not counted ('-outFilterMultimapNmax 1') since
298 they cannot be assigned to any gene unambiguously. In order to determine the differentially
299 expressed (DE) genes, generated BAM files were accessed with Cuffdiff (68), a program included
300 in Cufflinks. Cuffdiff reports reads per kp per million mapped reads (RPKM), \log_2 fold change,
301 together with *p*-value, and adjusted *p*-values (*q*-values). After Benjamini-Hochberg false discovery
302 correction, genes with *q*-values less than 0.05 were considered as DE genes. To examine sexual
303 differences, RPKM of DE vomeronasal receptor genes in male and female HR and Control mice
304 were subjected to two-way ANOVA tests using Prism (GraphPad). Notably, *p*-values for linetype-
305 biased expression of 4 DE receptor genes (Vmnr2r13, Vmnr2r23, Vmnr2r45, and Vmnr2r107) were >
306 0.05 due to differences of statistical tests: the negative binomial regression in DE gene detection
307 and the general linear model in two-way ANOVA.

308

309 Analysis of all-or-none SNPs

310 SNP data in supplemental table 7 (Data_S7) in Xu and Garland (2017) (50) were used for
311 this analysis. SNPs that separate all 4 HR and 4 Control lines (which we term all-or-none SNPs)
312 were selected (Supplemental Table 1) and mapped onto mouse genome (NCBI37/mm9) using
313 UCSC Genome Browser (<https://genome.ucsc.edu>). We noticed that most of the all-or-none SNPs
314 occurred in groups. Thus, we mapped those SNP clusters onto genomes (Supplemental Figure

315 3A). Each cluster was defined - and + 0.1 Mb from the first and last SNP, respectively, observed
316 in a specific location of the genome. Information of coding genes in each SNP cluster were
317 extracted (Supplemental Figure 3B). For some clusters, Gene-to-GO mappings was performed
318 with PANTHER (<http://pantherdb.org>).

319

320 RNAscope *in situ* hybridization

321 Female mice (11 Controls and 10 HRs) were utilized for this analysis. The animals were
322 intracardially perfused with 4% Paraformaldehyde in Phosphate Buffered Saline (PBS). VNOs
323 were dissected from perfused animals and fixed overnight. The VNO samples were decalcified in
324 EDTA pH 8.0 for 48 hours, then cryoprotected in 15% sucrose in PBS followed by 30% sucrose in
325 PBS. All samples were ultimately embedded in optimal cutting temperature (OCT) medium
326 (Electron Microscopy Sciences) above liquid nitrogen and sectioned at 20 μ m using Leica
327 CM3050S Cryostat. The cross sections analyzed were from the VNO regions with clearly
328 discernible two crescent shapes. They were collected approximately 120 μ m apart from each other
329 spanning approximately 360 μ m of the VNO containing regions from each mouse. Slides were
330 stored at -80°C until use for *in situ* hybridization staining.

331 RNA detection in VNOs were performed with ACD RNAscope® control and target
332 GNAO1 (ACD # and FPR3 (ACD #503451) using RNAscope® Multiplex Fluorescent Reagent
333 Kit v2 (ACD# 323100) Assay. Probe binding was detected with Akoya Biosciences' Opal 690
334 (FP1497001KT) and 570 (FP1488001KT) Dyes at 1:750 dilution in RNAscope TSA Buffer.
335 Nuclear staining was visualized with DAPI (EMS #17989-20). Images were acquired at 20X or
336 40X magnification on Zeiss Axio Imager.M2, and FPR3-positivity was quantified with a

337 proprietary script using QuPath software (69). Fluorescent intensity was measured by Fiji
338 software. 4-8 slices in each animal were examined. Mann-Whitney test was used to examine
339 statistical significance in Figure 5C and E.

340

341 **Acknowledgments**

342 We thank Drs C. R. Yu, H. Matsunami, T. Girke, P. Campbell, C. A. Scott and N. Yamanaka for
343 helpful discussions and comments on the manuscript. We are grateful for technical assistance from
344 Office of Campus Veterinarian, and Genomics Core Facility at University of California, Riverside
345 (UCR). This work was supported by UCR Initial Complement fund to S.H.Y., and NSF grant
346 DEB-1655362 to T.G.

347

348 **Author contributions**

349 S.H.Y. and T.G. designed the project. Q.A.N., D.H., and C.P. performed experiments. Q.A.N.,
350 S.K., T.H., T.G. and S.H.Y analyzed data. S.H.Y wrote the manuscript with comments from all
351 authors.

352

353 **Figure Legends**

354 Figure 1. RNAseq analysis of the vomeronasal organs of High Runner and Control mice
355 Heatmap of differentially expressed (DE) genes between HR and Control lines. DE vomeronasal
356 receptors are shown in red. Fpr3 (analyzed in Figure 4) is highlighted with a red underline.

357

358 Figure 2. RPKM comparison of DE vomeronasal receptors between High Runner and Control
359 mice

360 (A) Scatter plots showing the RPKM of DE vomeronasal receptor genes in each line of HR or C
361 mice. Black bars represent medians. (E) Bar graph denoting \log_2 fold change of the relative
362 expression of DE vomeronasal receptor genes between the HR and Control lines.

363

364 Figure 3. Chromosomal locations of DE vomeronasal receptors

365 A plot showing the \log_2 fold change of 336 vomeronasal receptor genes in their relative positions
366 along the chromosomes. Each circle represents a member of *Vmn1r*, *Vmn2r*, or *Fpr* family genes.
367 DE vomeronasal receptors are shown in filled circles.

368

369 Figure 4. A genomic cluster containing both SNPs and DE vomeronasal receptors

370 (A) A genomic cluster containing DE vomeronasal receptor genes in the mouse chromosomes 17.
371 Vomeronasal receptors in red and blue indicate up- and down-regulations, respectively. Non-DE
372 genes are shown in black. Purple arrowheads indicate locations of SNPs that are significantly
373 differentiated between HR and Control groups (50), as shown in a table (B).

374

375 Figure 5. RNA scope *in situ* hybridization analysis of a DE vomeronasal receptor gene in the VNO
376 (A) Images showing RNAscope-derived fluorescent signals for *Fpr3* (left) and *Gnao1* (middle)
377 transcripts. In merged images (right), *Fpr3* and *Gnao1* are shown in red and yellow, respectively,

378 together with DAPI staining (blue). Upper and lower panels show representative images from the
379 VNO of a Control (line 5) line and a HR (line 3) line, respectively. (B) A scatter plot showing the
380 number of *Fpr3* signals in 1,000 vomeronasal sensory neurons per VNO slice for each line of
381 mice. n = 12 slices in 2 - 3 mice per line. Black bars represent medians. (C) The mean number of
382 *Fpr3* signals in 1,000 VSNs in Control and HR lines. Each dot indicates the mean of one line.
383 Black bars represent medians. * indicates $p < 0.05$ in Mann-Whitney test. (D) Representative
384 images showing *Fpr3* signals (red) observed in the VNO of Control and HR lines of mice. DAPI
385 signals are shown in blue. (E) The mean of *Fpr3* signal intensity (arbitrary unit, AU) per VSN in
386 the Control and HR lines. Each dot indicates the mean of one line. Black bars represent medians.

387

388 Supplemental Figure 1. RPKM comparison of DE vomeronasal receptors between males and
389 females in High Runner and Control mice

390 Scatter plots showing the RPKM of DE *vomeronasal receptor* genes in males and females from
391 each line of HR or Control mice. Black bars represent medians.

392

393 Supplemental Figure 2. Two-way ANOVA tests of DE vomeronasal receptors

394 A table showing p -values for interactions, sex differences, and linetype differences in the RPKM
395 of DE vomeronasal receptor genes in two-way ANOVA analyses. n.s., *, **, ***, and ****
396 represent not significant, $p < 0.05$, $p < 0.01$, $p < 0.001$, and $p < 0.0001$, respectively.

397

398 Supplemental Figure 3. Analysis of all-or-none SNP loci in HR and Control lines of mice

399 (A) A schematic diagram showing the relative positions of loci containing 1 or more all-or-none
400 SNPs. Blue triangles indicate non-chemosensory clusters, and a red triangle indicates clusters
401 containing only chemosensory (vomeronasal) receptors. (B) A table showing chromosomal
402 location and length of each all-or-non SNP cluster, and the number of SNPs and genes within the
403 clusters. The row highlighted in red is the cluster containing only the vomeronasal receptor genes.

404

405 Supplemental Table 1.

406 Genomic locations, *p*-value by the mixed model approach (50), and allele frequencies of the 61
407 all-or-on SNP loci.

408

409 **References**

410

411 1. Nielsen BL. Olfaction in animal behaviour and welfare: CABI; 2017 2017/6/29. 233 p.

412 2. Liberles SD. Mammalian pheromones. *Annu Rev Physiol.* 2014;76:151-75.

413 3. Mohrhardt J, Nagel M, Fleck D, Ben-Shaul Y, Spehr M. Signal Detection and Coding in the
414 Accessory Olfactory System. *Chem Senses.* 2018;43(9):667-95.

415 4. Ishii KK, Touhara K. Neural circuits regulating sexual behaviors via the olfactory system in
416 mice. *Neurosci Res.* 2019;140:59-76.

417 5. Fleischer J, Krieger J. Insect Pheromone Receptors - Key Elements in Sensing Intraspecific
418 Chemical Signals. *Front Cell Neurosci.* 2018;12:425.

419 6. Cande J, Prud'Homme B, Gompel N. Smells like evolution: the role of chemoreceptor
420 evolution in behavioral change. *Curr Opin Neurobiol.* 2013;23(1):152-8.

421 7. Liberles SD. Mammalian pheromones. *Annu Rev Physiol.* 2014;76(1):151-75.

422 8. Halpern M. The organization and function of the vomeronasal system. *Annu Rev Neurosci*
423 1987;10(1):325-62.

424 9. Halpern M. Structure and function of the vomeronasal system: an update. *Prog Neurobiol.*
425 2003;70(3):245-318.

426 10. Dulac C, Axel R. A novel family of genes encoding putative pheromone receptors in
427 mammals. *Cell.* 1995;83(2):195-206.

428 11. Herrada G, Dulac C. A novel family of putative pheromone receptors in mammals with a
429 topographically organized and sexually dimorphic distribution. *Cell.* 1997;90(4):763-73.

430 12. Matsunami H, Buck LB. A multigene family encoding a diverse array of putative pheromone
431 receptors in mammals. *Cell.* 1997;90(4):775-84.

432 13. Rivière S, Challet L, Fluegge D, Spehr M, Rodriguez I. Formyl peptide receptor-like proteins
433 are a novel family of vomeronasal chemosensors. *Nature.* 2009;459(7246):574-7.

434 14. Liberles SD, Horowitz LF, Kuang D, Contos JJ, Wilson KL, Siltberg-Liberles J, et al. Formyl
435 peptide receptors are candidate chemosensory receptors in the vomeronasal organ. *Proc Natl
436 Acad Sci U S A.* 2009;106(24):9842-7.

437 15. Wagner S, Gresser AL, Torello AT, Dulac C. A multireceptor genetic approach uncovers an
438 ordered integration of VNO sensory inputs in the accessory olfactory bulb. *Neuron.*
439 2006;50(5):697-709.

440 16. Ben-Shaul Y, Katz LC, Mooney R, Dulac C. In vivo vomeronasal stimulation reveals sensory
441 encoding of conspecific and allospecific cues by the mouse accessory olfactory bulb. *Proc Natl
442 Acad Sci U S A.* 2010;107(11):5172-7.

443 17. Meredith M. Vomeronasal, Olfactory, Hormonal Convergence in the Brain: Cooperation or
444 Coincidence? *Ann N Y Acad Sci.* 1998;855(1 OLFACTION AND):349-61.

445 18. Tirindelli R, Dibattista M, Pifferi S, Menini A. From pheromones to behavior. *Physiol Rev.*
446 2009;89(3):921-56.

447 19. Wynn EH, Sánchez-Andrade G, Carss KJ, Logan DW. Genomic variation in the vomeronasal
448 receptor gene repertoires of inbred mice. *BMC Genomics.* 2012;13:415.

449 20. Zhang J, Webb DM. Evolutionary deterioration of the vomeronasal pheromone transduction
450 pathway in catarrhine primates. *Proc Natl Acad Sci U S A.* 2003;100(14):8337-41.

451 21. Grus WE, Zhang J. Rapid turnover and species-specificity of vomeronasal pheromone receptor
452 genes in mice and rats. *Gene.* 2004;340(2):303-12.

453 22. Shi P, Bielawski JP, Yang H, Zhang Y-P. Adaptive diversification of vomeronasal receptor 1
454 genes in rodents. *J Mol Evol.* 2005;60(5):566-76.

455 23. Shi P, Zhang J. Comparative genomic analysis identifies an evolutionary shift of vomeronasal
456 receptor gene repertoires in the vertebrate transition from water to land. *Genome Res.*
457 2007;17(2):166-74.

458 24. Grus WE, Zhang J. Origin of the genetic components of the vomeronasal system in the
459 common ancestor of all extant vertebrates. *Mol Biol Evol.* 2009;26(2):407-19.

460 25. Grus WE, Zhang J. Origin and evolution of the vertebrate vomeronasal system viewed through
461 system-specific genes. *Bioessays.* 2006;28(7):709-18.

462 26. Grus WE, Shi P, Zhang J. Largest vertebrate vomeronasal type 1 receptor gene repertoire in
463 the semiaquatic platypus. *Mol Biol Evol.* 2007;24(10):2153-7.

464 27. Young JM, Trask BJ. V2R gene families degenerated in primates, dog and cow, but expanded
465 in opossum. *Trends Genet.* 2007;23(5):212-5.

466 28. Young JM, Massa HF, Hsu L, Trask BJ. Extreme variability among mammalian V1R gene
467 families. *Genome Res.* 2010;20(1):10-8.

468 29. Young JM. Divergent V1R repertoires in five species: Amplification in rodents, decimation in
469 primates, and a surprisingly small repertoire in dogs. *Genome Res.* 2005;15(2):231-40.

470 30. Lane RP, Cutforth T, Axel R, Hood L, Trask BJ. Sequence analysis of mouse vomeronasal
471 receptor gene clusters reveals common promoter motifs and a history of recent expansion. *Proc
472 Natl Acad Sci.* 2002;99(1):291-6.

473 31. Lane RP, Young J, Newman T, Trask BJ. Species specificity in rodent pheromone receptor
474 repertoires. *Genome Res.* 2004;14(4):603-8.

475 32. Yang H, Shi P, Zhang Y-P, Zhang J. Composition and evolution of the V2r vomeronasal
476 receptor gene repertoire in mice and rats. *Genomics.* 2005;86(3):306-15.

477 33. Couger MB, Arévalo L, Campbell P. A high quality genome for *mus spicilegus*, a close
478 relative of house mice with unique social and ecological adaptations. *G3.* 2018;8(7):2145-52.

479 34. Grus WE, Shi P, Zhang YP, Zhang J. Dramatic variation of the vomeronasal pheromone
480 receptor gene repertoire among five orders of placental and marsupial mammals. *Proc Natl
481 Acad Sci.* 2005;102(16):5767-72.

482 35. Duyck K, DuTell V, Ma L, Paulson A, Yu CR. Pronounced strain-specific chemosensory
483 receptor gene expression in the mouse vomeronasal organ. *BMC Genomics*. 2017;18(1):965.

484 36. Meijer JH, Robbers Y. Wheel running in the wild. *Proc Biol Sci*. 2014;281(1786).

485 37. Sherwin CM. Voluntary wheel running: a review and novel interpretation. *Anim Behav*.
486 1998;56(1):11-27.

487 38. Garland T, Jr., Schutz H, Chappell MA, Keeney BK, Meek TH, Copes LE, et al. The
488 biological control of voluntary exercise, spontaneous physical activity and daily energy
489 expenditure in relation to obesity: human and rodent perspectives. *The Journal of experimental*
490 *biology*. 2011;214(Pt 2):206-29.

491 39. Novak CM, Burghardt PR, Levine JA. The use of a running wheel to measure activity in
492 rodents: relationship to energy balance, general activity, and reward. *Neuroscience and*
493 *biobehavioral reviews*. 2012;36(3):1001-14.

494 40. Lightfoot JT, EJC DEG, Booth FW, Bray MS, M DENH, Kaprio J, et al. Biological/Genetic
495 Regulation of Physical Activity Level: Consensus from GenBioPAC. *Med Sci Sports Exerc*.
496 2018;50(4):863-73.

497 41. Rhodes JS, Gammie SC, Garland T, Jr. Neurobiology of mice selected for high voluntary
498 wheel-running activity. *Integrative and comparative biology*. 2005;45(3):438-55.

499 42. Claghorn GC, Thompson Z, Wi K, Van L, Garland T, Jr. Caffeine stimulates voluntary wheel
500 running in mice without increasing aerobic capacity. *Physiol Behav*. 2017;170:133-40.

501 43. Drickamer LC, Evans TR. Chemosignals and activity of wild stock house mice, with a note on
502 the use of running wheels to assess activity in rodents. *Behav Processes*. 1996;36(1):51-66.

503 44. Swallow JG, Carter PA, Garland T, Jr. Artificial selection for increased wheel-running
504 behavior in house mice. *Behav Genet*. 1998;28(3):227-37.

505 45. Wallace IJ, Garland T, Jr. Mobility as an emergent property of biological organization:
506 Insights from experimental evolution. *Evol Anthropol*. 2016;25(3):98-104.

507 46. Kolb EM, Kelly SA, Garland T, Jr. Mice from lines selectively bred for high voluntary wheel
508 running exhibit lower blood pressure during withdrawal from wheel access. *Physiol Behav*.
509 2013;112-113:49-55.

510 47. Careau V, Wolak ME, Carter PA, Garland T. Limits to behavioral evolution: the quantitative
511 genetics of a complex trait under directional selection. *Evolution*. 2013;67(11):3102-19.

512 48. Dewan I, Garland T, Hiramatsu L, Careau V. I smell a mouse: indirect genetic effects on
513 voluntary wheel-running distance, duration and speed. *Behavior Genetics*. 2019;49(1):49-59.

514 49. Kream RM, Margolis FL. Olfactory marker protein: turnover and transport in normal and
515 regenerating neurons. *J Neurosci*. 1984;4(3):868-79.

516 50. Xu S, Garland T. A mixed model approach to genome-wide association studies for selection
517 signatures, with application to mice bred for voluntary exercise behavior. *Genetics*.
518 2017;207(2):785-99.

519 51. Khan M, Vaes E, Mombaerts P. Regulation of the probability of mouse odorant receptor gene
520 choice. *Cell*. 2011;147(4):907-21.

521 52. Hillis DA, Yadgary L, Weinstock GM, Pardo-Manuel de Villena F, Pomp D, Fowler AS, et al.
522 Genetic Basis of Aerobically Supported Voluntary Exercise: Results from a Selection
523 Experiment with House Mice. *Genetics*. 2020.

524 53. Kolb EM, Rezende EL, Holness L, Radtke A, Lee SK, Obenaus A, et al. Mice selectively bred
525 for high voluntary wheel running have larger midbrains: support for the mosaic model of brain
526 evolution. *The Journal of experimental biology*. 2013;216(3):515-23.

527 54. Swallow JG, Rhodes JS, Garland T, Jr. Phenotypic and evolutionary plasticity of organ masses
528 in response to voluntary exercise in house mice. *Integr Comp Biol*. 2005;45(3):426-37.

529 55. Kelly SA, Gomes FR, Kolb EM, Malisch JL, Garland T, Jr. Effects of activity, genetic
530 selection and their interaction on muscle metabolic capacities and organ masses in mice. *The
531 Journal of experimental biology*. 2017;220(Pt 6):1038-47.

532 56. Kolb EM, Kelly SA, Middleton KM, Sermsakdi LS, Chappell MA, Garland T. Erythropoietin
533 elevates but not voluntary wheel running in mice. 2010;213(3):510-9.

534 57. Kay JC, Claghorn GC, Thompson Z, Hampton TG, Garland T, Jr. Electrocardiograms of mice
535 selectively bred for high levels of voluntary exercise: Effects of short-term exercise training
536 and the mini-muscle phenotype. *Physiol Behav*. 2019;199:322-32.

537 58. Rezende EL, Gomes FR, Malisch JL, Chappell MA, Garland T, Jr. Maximal oxygen
538 consumption in relation to subordinate traits in lines of house mice selectively bred for high
539 voluntary wheel running. *J Appl Physiol*. 2006;101(2):477-85.

540 59. Haga S, Hattori T, Sato T, Sato K, Matsuda S, Kobayakawa R, et al. The male mouse
541 pheromone ESP1 enhances female sexual receptive behaviour through a specific vomeronasal
542 receptor. *Nature*. 2010;466(7302):118-22.

543 60. Ferrero DM, Moeller LM, Osakada T, Horio N, Li Q, Roy DS, et al. A juvenile mouse
544 pheromone inhibits sexual behaviour through the vomeronasal system. *Nature*.
545 2013;502(7471):368-71.

546 61. Cheetham SA, Smith AL, Armstrong SD, Beynon RJ, Hurst JL. Limited variation in the major
547 urinary proteins of laboratory mice. *Physiol Behav*. 2009;96(2):253-61.

548 62. Rhodes JS, Garland T, Jr., Gammie SC. Patterns of brain activity associated with variation in
549 voluntary wheel-running behavior. *Behav Neurosci*. 2003;117(6):1243-56.

550 63. King JM. Effects of lesions of the amygdala, preoptic area, and hypothalamus on estradiol-
551 induced activity in the female rat. *Journal of comparative and physiological psychology*.
552 1979;93(2):360-7.

553 64. Fahrbach S, Meisel R, Pfaff D. Preoptic implants of estradiol increase wheel running but not
554 the open field activity of female rats. 1985;35(6):985-92.

555 65. Ogawa S, Chan J, Gustafsson J-Å, Korach KS, Pfaff DW. Estrogen Increases Locomotor
556 Activity in Mice through Estrogen Receptor α : Specificity for the Type of Activity.
557 *Endocrinology*. 2003;144(1):230-9.

558 66. Spiteri T, Ogawa S, Musatov S, Pfaff DW, Ågmo A. The role of the estrogen receptor α in the
559 medial preoptic area in sexual incentive motivation, proceptivity and receptivity, anxiety, and
560 wheel running in female rats. 2012;230(1):11-20.

561 67. Dobin A, Davis CA, Schlesinger F, Drenkow J, Zaleski C, Jha S, et al. STAR: ultrafast
562 universal RNA-seq aligner. Bioinformatics. 2013;29(1):15-21.

563 68. Trapnell C, Hendrickson DG, Sauvageau M, Goff L, Rinn JL, Pachter L. Differential analysis
564 of gene regulation at transcript resolution with RNA-seq. Nat Biotechnol. 2013;31(1):46-53.

565 69. Bankhead P, Loughrey MB, Fernandez JA, Dombrowski Y, McArt DG, Dunne PD, et al.
566 QuPath: Open source software for digital pathology image analysis. Sci Rep. 2017;7(1):16878.

567

Figure 1

Click here to access/download;Figure;Fig 1.eps

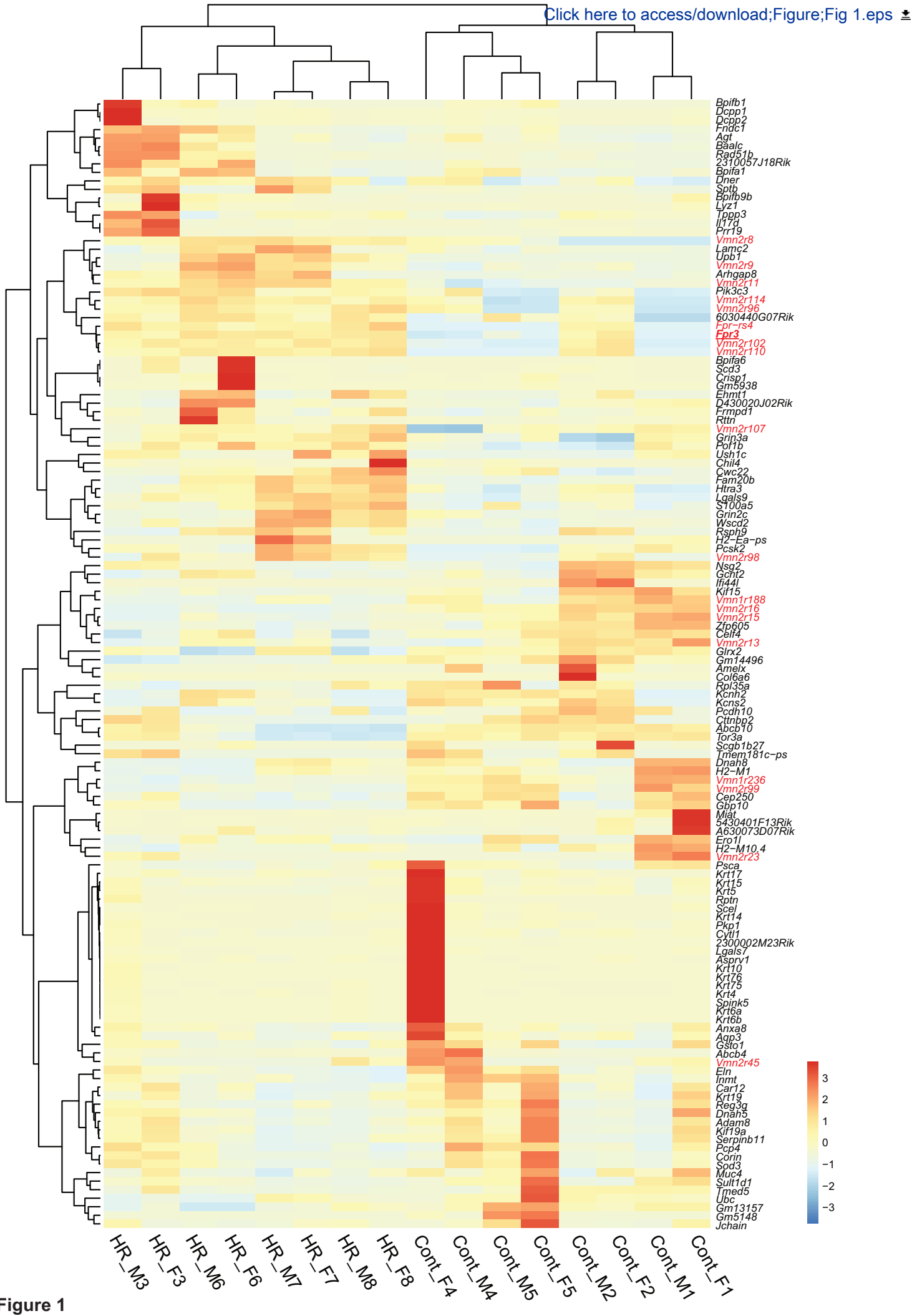
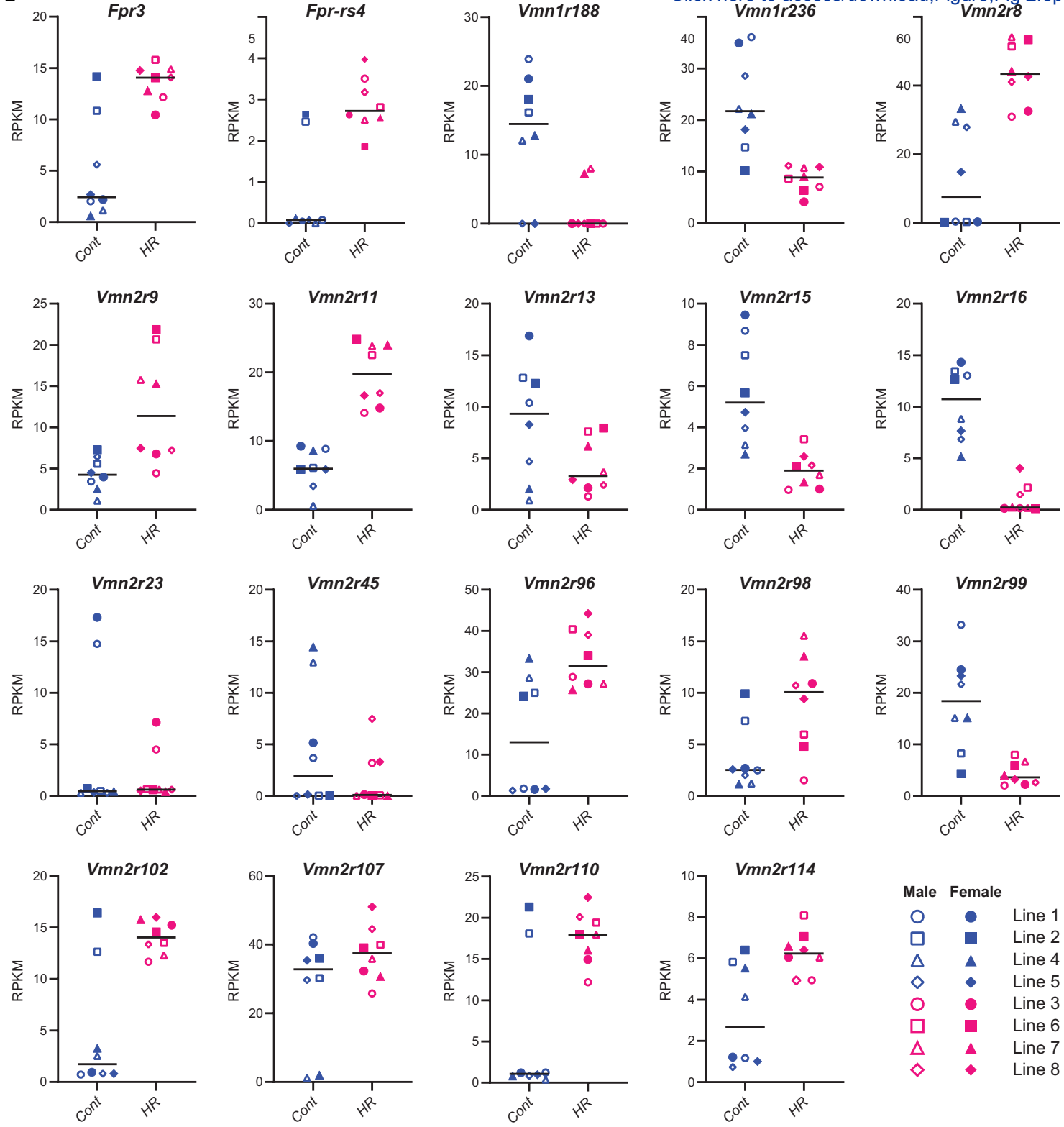
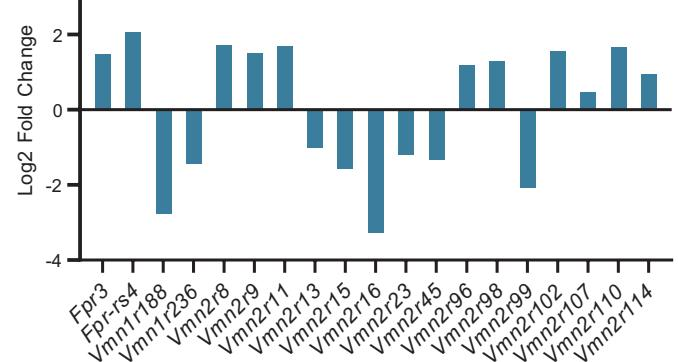


Figure 1

Figure A2[Click here to access/download;Figure;Fig 2.eps](#)**B****Figure 2**

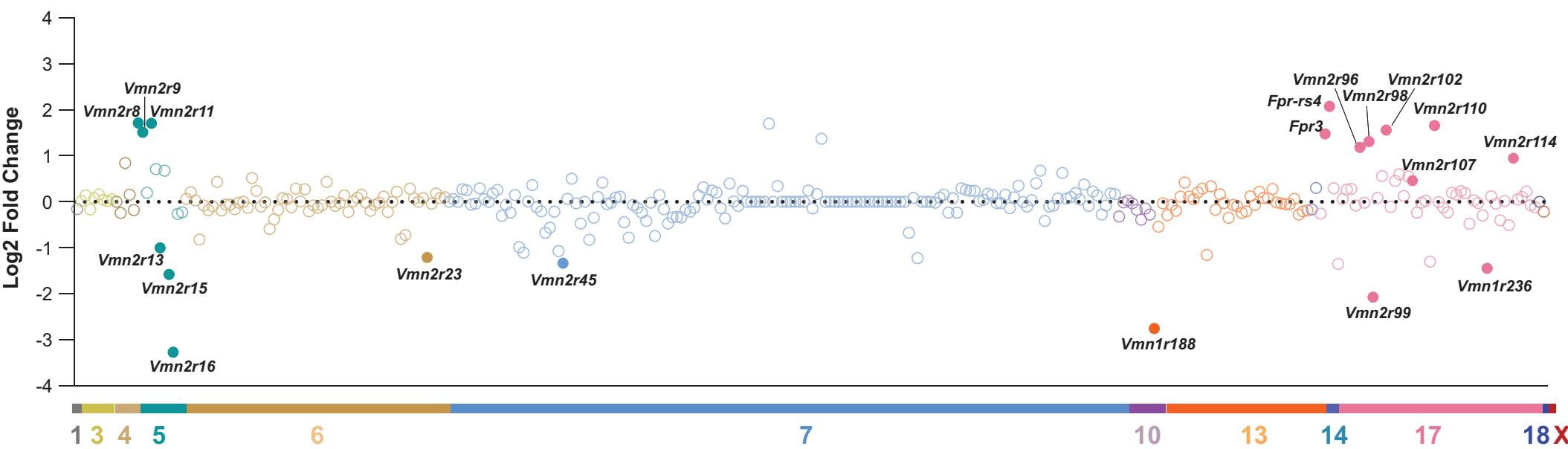
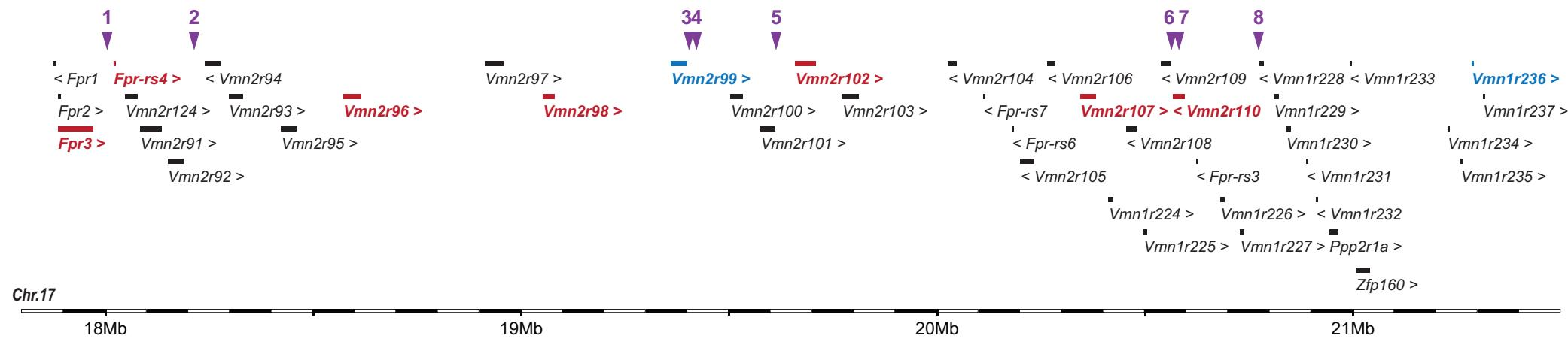


Figure 3

Figure 4

Click here to access/download;Figure;Fig 4.eps

A



B

	SNP ID	SNP location (mm10)	HR / Cont	Gene (within 50kb)	strand	up/dw	Distance (bp)
1	rs29503987	18001459	C / A	<i>Fpr-3</i>	+	dw	29935
				<i>Fpr-rs4</i>	+	up	20274
				<i>Vmn2r124</i>	+	up	48025
2	rs33375308	18210739	T / C	<i>Vmn2r92</i>	+	dw	25561
3	rs33447983	19403011	G / T	<i>Vmn2r99</i>	+	dw	8421
4	rs6224641	19424358	A / G	<i>Vmn2r99</i>	+	dw	29768
5	rs33649277	19616228	G / A	<i>Vmn2r101</i>	+	dw	3911
				<i>Vmn2r102</i>	+	up	44171
6	rs29522462	20573305	A / C	<i>Vmn2r109</i>	-	up	8549
				<i>Vmn2r110</i>	-	dw	524
7	rs33120398	20587484	C / T	<i>Vmn2r109</i>	-	up	22728
				<i>Vmn2r110</i>	-	intron 1	
				<i>Fpr-rs3</i>	-	dw	36362
8	rs33463529	20779567	G / A	<i>Vmn1r227</i>	+	dw	43441
				<i>Vmn1r228</i>	-	up	2066
				<i>Vmn1r229</i>	+	up	34928

Figure 4

Figure 5

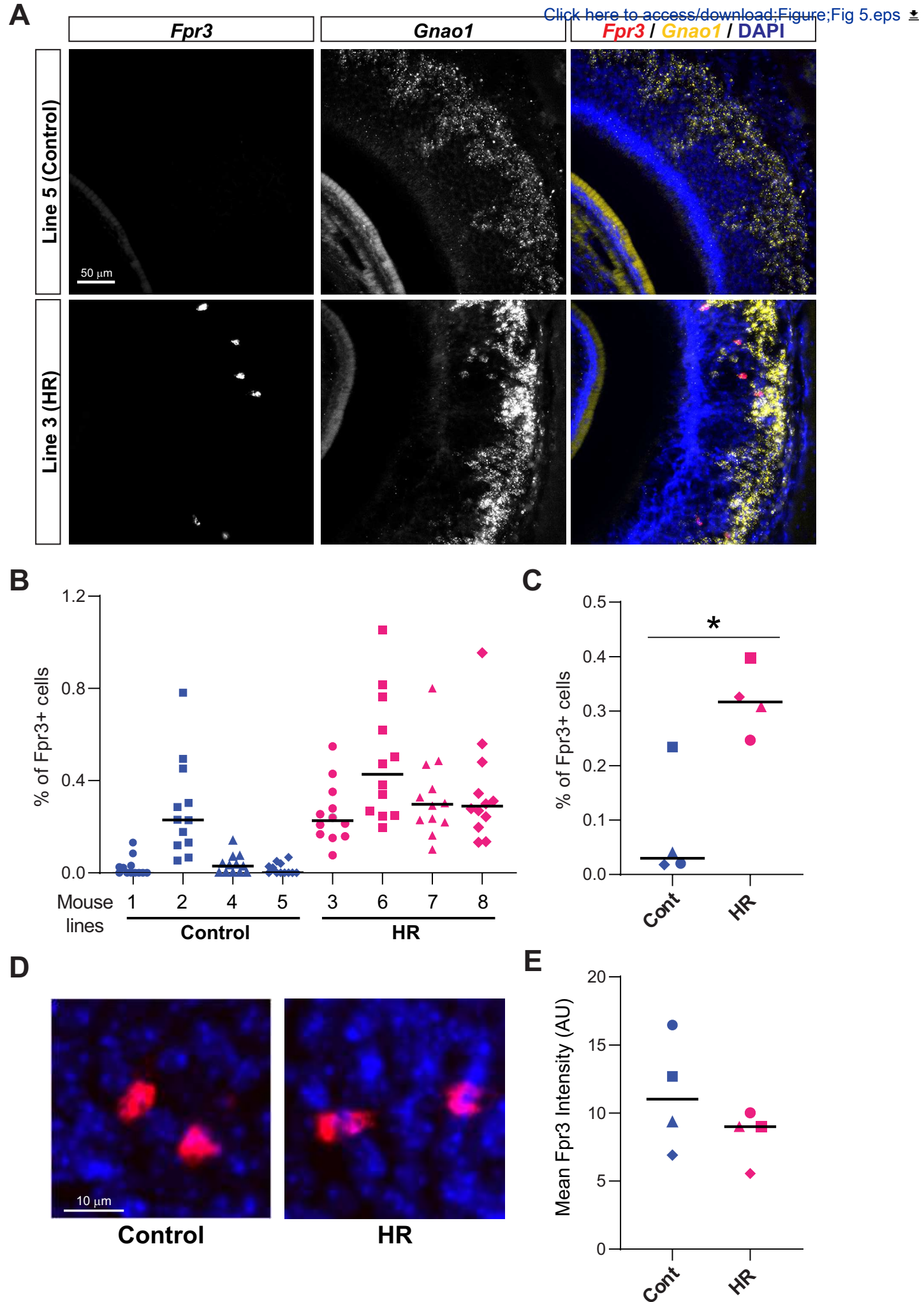


Figure 5



Click here to access/download
Supporting Information
Supplement Fig 1.eps





Click here to access/download
Supporting Information
Supplement Fig 2.eps





Click here to access/download
Supporting Information
Supplement Fig 3.eps





Click here to access/download
Supporting Information
Supplemental Table 1-20200427.xlsx